ARTICLE

Check for updates

Journal of
Sensor Science and Technology

The Korean Sensors Society

Advanced Stirling Generator Testing System with High Sampling Frequency

Gujin Kang[1], Kilyoung Ko[1], Jongbum Kim[1], Jin-Joo Kim[1], Sunjin Kim[1], Jintae Hong[1,+], and Yongrok Jeong[2,+]

[1]*Radioisotope Research Division, Korea Atomic Energy Research Institute, 111 Daedeok-daero 989beon-gil, Yuseong-gu, Daejeon, 34057, Republic of Korea*
[2]*School of Mechanical Engineering, Kyungpook National University, 80 Daehak-ro, Buk-gu, Daejeon, 41566, Republic of Korea*

Cite This: *J. Sens. Sci. Technol. Vol. 34, No. 6 (2025) 623-629*

https://doi.org/10.46670/JSST.2025.34.6.623

ABSTRACT: This study presents the design and validation of an integrated monitoring and control system for a laboratory-scale Stirling generator. Conventional testbeds suffer from unsynchronized, low-bandwidth data acquisition, which hinders the real-time analysis of dynamic parameters such as internal pressure, piston motion, and electrical output. To overcome these limitations, a modular platform was developed that integrates precise helium pressure control, temperature gradient management, and high-speed data acquisition synchronized via a LabView interface. The system enables real-time monitoring of multiple variables, including temperature, pressure, AC voltage, AC current, and DC voltage/current, at sampling rates up to 2 kHz. Experimental validation was conducted using a lab-scale Stirling generator fabricated in a previous study under optimized driving conditions. During two-hour continuous operation, the output power stabilized at 4.51 W, representing a 6% decrease from the initial 4.80 W with a deviation of less than 1%. Amplitude sweep tests revealed a performance threshold at approximately 7.8V, where a drop in current indicated a piston-gas mismatch at excessive amplitudes. These results confirm the capability of the platform for accurate and synchronized monitoring. The developed system established a robust foundation for the dynamic characterization and control of Stirling generators toward high-efficiency, long-endurance power generation in extreme environments.

KEYWORDS: *Stirling generator, High sampling frequency, Lab-scale measurement setup, Real-time monitoring*

1. INTRODUCTION

Stirling engines have emerged as promising candidates for reliable and efficient power generation strategies in both terrestrial and space-constrained environments owing to their high closed-cycle operation, high thermal-to-electrical energy transformation efficiency, multi-fuel capability, and low noise characteristics [1-6]. With the increasing demand for long-endurance unmanned platforms and extreme-environment energy systems, the need for stable and optimally controlled Stirling engines has become increasingly prominent [7].

However, conventional Stirling engine testbeds often rely on fragmented, low-bandwidth measurement setups that are not designed for real-time synchronized data acquisition [8-9]. This presents a significant challenge in high-frequency operation modes, such as those observed in free-piston Stirling engines, where the ability to precisely monitor and analyze the phase relationships between key parameters is crucial. Specifically, the real-time correlation of internal pressure oscillations, piston vibrations, and electrical output waveforms is rarely achievable in traditional setups because of fragmented measurement setups and inadequate sampling rates. These limitations hinder dynamic performance analysis, impede fault detection, and restrict the development of advanced control algorithms.

To address these challenges, we developed an integrated monitoring and control system tailored to a laboratory-scale Stirling engine. The system consists of an AC power supply for generator kick-off and stabilization, a DC power supply for operating the Joule heater used as a heat source for the Stirling engine, a helium pressure regulation unit for precise helium filling of the Stirling engine, and a modular data acquisition (DAQ) system capable of multichannel high-speed

[+]Corresponding authors: jthong@kaeri.re.kr, yongrok@knu.ac.kr
Received : Oct. 15, 2025, Revised : Oct. 20, 2025, Accepted : Oct. 23, 2025

This is an Open Access article distributed under the terms of the Creative Commons Attribution Non-Commercial License (https://creativecommons.org/licenses/by-nc/3.0/) which permits unrestricted non-commercial use, distribution, and reproduction in any medium, provided the original work is properly cited.

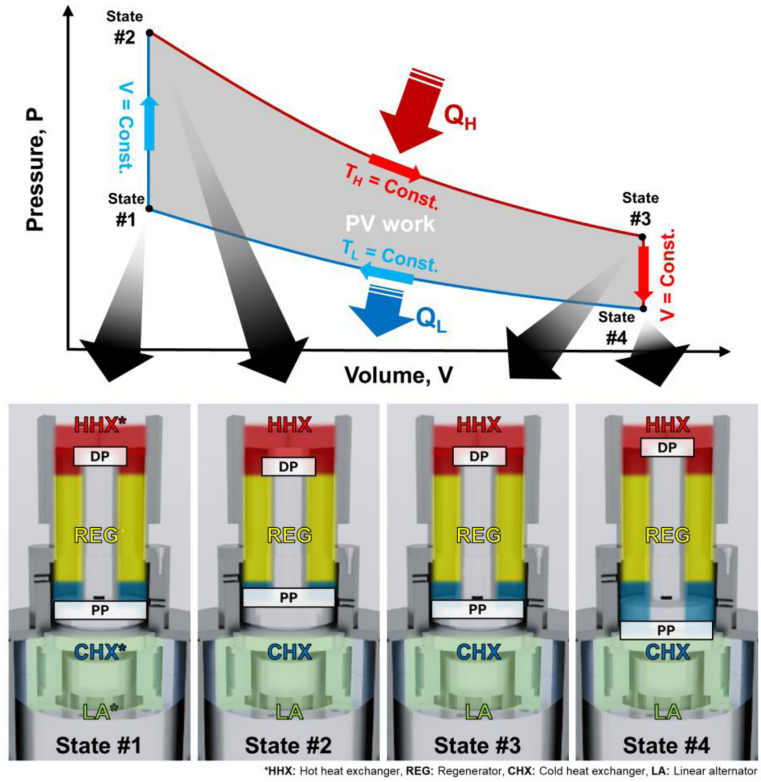

Fig. 1. Principle of the Stirling generator.

sampling. This paper presents the detailed architecture of the system, describes its implementation process, and outlines a data acquisition strategy for accurate real-time monitoring.

2. SYSTEM DETAIL

2.1 Stirling Generator Background

A Stirling generator is a device that converts acoustic waves generated by thermal energy into mechanical vibrations and subsequently into electrical energy using a linear alternator. The conversion process can be described using the Stirling thermodynamic cycle, as shown in Fig. 1. Theoretically, the Stirling generator can achieve efficiencies close to the Carnot limit, indicating its high potential for practical applications once the technology is fully developed. In particular, when designed as a Free-Piston Stirling Engine (FPSE), the generator can be completely hermetically sealed while still operating as an external combustion engine, thereby providing significant advantages for deployment in extreme environments. Therefore, FPSE systems have been developed and applied in the United States and China for space- and defense-related power generation, and similar efforts are ongoing at the Korea Atomic Energy Research Institute (KAERI). The prototype Stirling generator used in this study was developed by KAERI and reported by Jeong et al. [10]. Under the conditions of 63.7 Hz operating frequency, 15.4 atm helium pressure, heater temperature of 600°C, and 5 V amplitude, the prototype achieved a maximum output of 3.05 W, corresponding to a reported efficiency of 4.15%.

The operation of a Stirling generator requires a sufficient temperature gradient (ΔT). Consequently, such systems are typically integrated with waste-heat recovery units [11] or solar concentrators [4] capable of providing a large ΔT. In the experimental environment proposed in this study, the hot end was controlled using an electric resistance heater, and the cold end was maintained using a water-cooled chiller system to achieve precise ΔT control. In addition, the type and pressure of the working fluid significantly influence the performance; therefore, an internal pressure control system consisting of a vacuum pump, pressure sensors, and an electronic regulator was implemented for accurate adjustment.

2.2 Hardware System

The test bench for the Stirling engine is broadly divided into two subsystems: (1) an environmental condition setup for engine operation (Fig. 2(a, b), and (2) a monitoring system for engine performance during operation (Fig. 2(c)).

The environmental setup comprises two key functions: helium

ⓒ The Korean Sensors Society

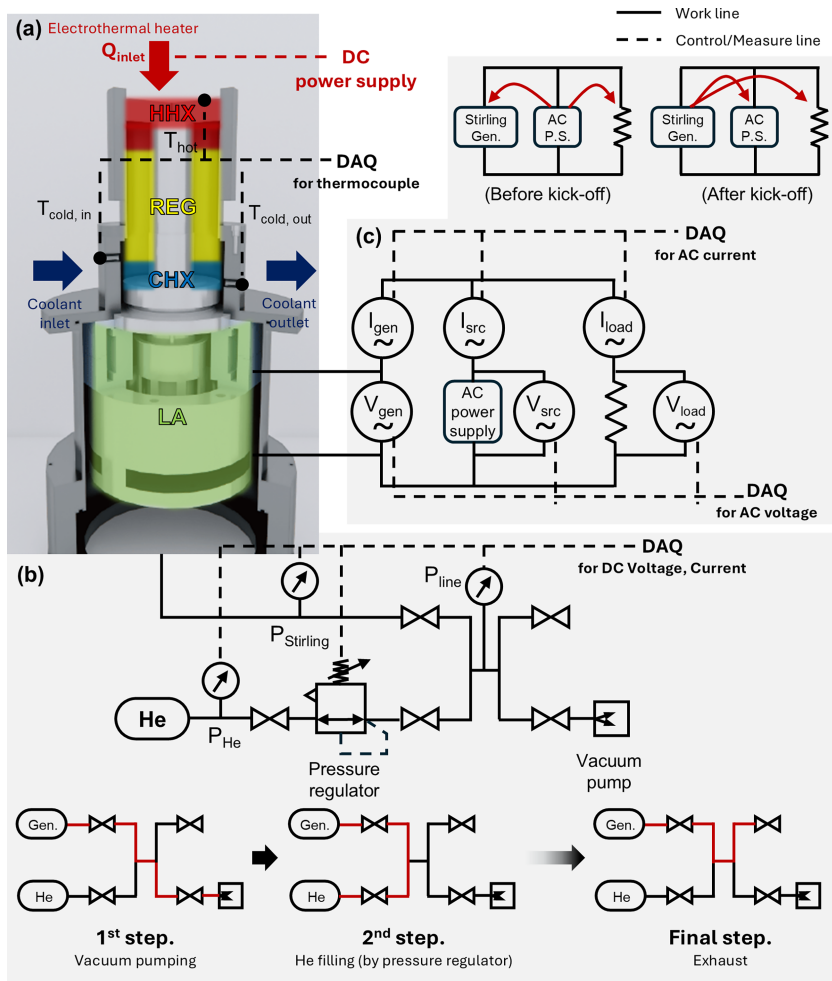

Fig. 2. Schematic of Stirling generator hardware; (a) Stirling generator, (b) Internal liquid control system, (c) Electrical power generating system.

charging and temperature gradient formation. Before starting the engine, helium as the working fluid must be charged into the engine at the target pressure, and two requirements must be satisfied: (1) no other gases should remain inside the engine, and (2) the charging pressure must be precisely controlled. To satisfy these requirements, an internal pressure control system was designed, as shown in Fig. 2(b), which connects the engine to three ports. The first port is linked to a vacuum pump to evacuate the chamber before helium charging. The second port is a helium line equipped with an electronic regulator (CHP-HFE-5GI, Clippard, USA), which enables accurate pressurization of the engine. The third port connects to the atmosphere and is used for exhaust during depressurization.

In practice, the system is first evacuated for approximately 30 min using a vacuum pump, after which helium is introduced from a high-pressure cylinder through a regulator. Pressure variations during this process are monitored using two types of sensors: one covers a wide pressure range, enabling monitoring throughout the entire charging process, and the other provides a sufficiently fast response to track pressure oscillations at the operating frequency of the engine, thereby capturing transient variations during engine operation.

A temperature gradient was established after helium charging. The hot end was heated using a custom-made Joule heater powered by a DC power supply (N6700C, Keithley, USA), and the cold end was cooled using a coolant circulator (RW3-1035, JEIO Tech, Republic of Korea).

The engine-monitoring system consists of an AC power supply for startup and stable operation, a DAQ setup for measurement, and an external load for power consumption (Fig. 2(c)). Once the ΔT is established, the AC power supply initiates engine operation, and the engine thereafter produces continuous power. During laboratory experiments, the generated power was dissipated through a resistive electrical load in actual applications, this load is replaced by power storage devices such as batteries or capacitors.

Impedance matching within a circuit is critical for ensuring stable operation. The high-frequency AC voltage and current signals from the AC power supply, Stirling engine, and electrical load were monitored to calculate the effective power output and

ⓒ The Korean Sensors Society

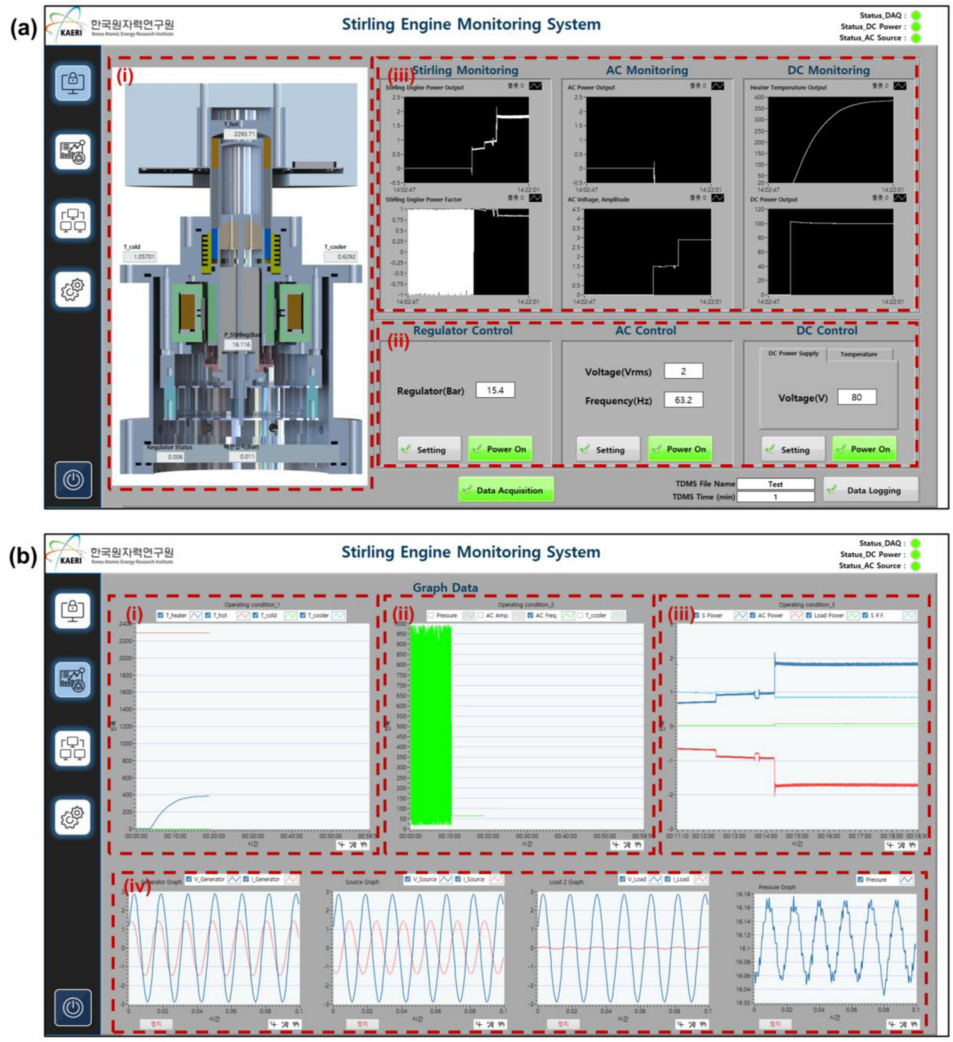

Fig. 3. Software interface for the Stirling generator; (a) System control interface, (b) System monitoring interface.

efficiency. In addition, multiple parameters, including the heater temperature, coolant inlet and outlet temperatures, internal helium pressure, AC voltages, AC currents, and electronic load state, were simultaneously monitored using the DAQ chassis (cDAQ-9189, National Instruments, USA). Specifically, an NI-9210 (National Instruments, USA) was used for temperature monitoring (8 CH), NI-9253 (National Instruments, USA) for DC current and pressure monitoring, NI-9225 (National Instruments, USA) for AC voltage monitoring (3 CH), and NI-9247 (National Instruments, USA) for AC current monitoring (3 CH). Furthermore, NI-9263 (National Instruments, USA) provided a DC voltage output (3 CH), whereas NI-9215 (National Instruments, USA) enabled DC voltage monitoring (4 CH), allowing regulator operation monitoring and future sensor integration.

2.3 Software System

Owing to the intrinsic dynamics of the Stirling engine, which are characterized by rapid piston motion, oscillatory pressure variations, and high-frequency voltage/current responses, the software system must be capable of synchronizing multiple hardware components while maintaining high monitoring frequencies. In this study, all hardware modules were integrated into a single LabView-based program. The software was organized into two main interfaces: one for system control and the other for detailed monitoring.

The system control interface (Fig. 3(a)) allows for the regulation of the helium charging pressure, AC power supply settings, and heater power input. The left display panel provides a schematic overview of the external environment of the Stirling engine, showing the hot- and cold-end temperatures, internal engine pressure, and pressure in the control system (Fig. 3(a-i)). The regulator can be operated through a dedicated controller (Fig. 3(a-ii)), whereas the Joule heater is controlled via a DC input panel that also displays the

ⓒ The Korean Sensors Society

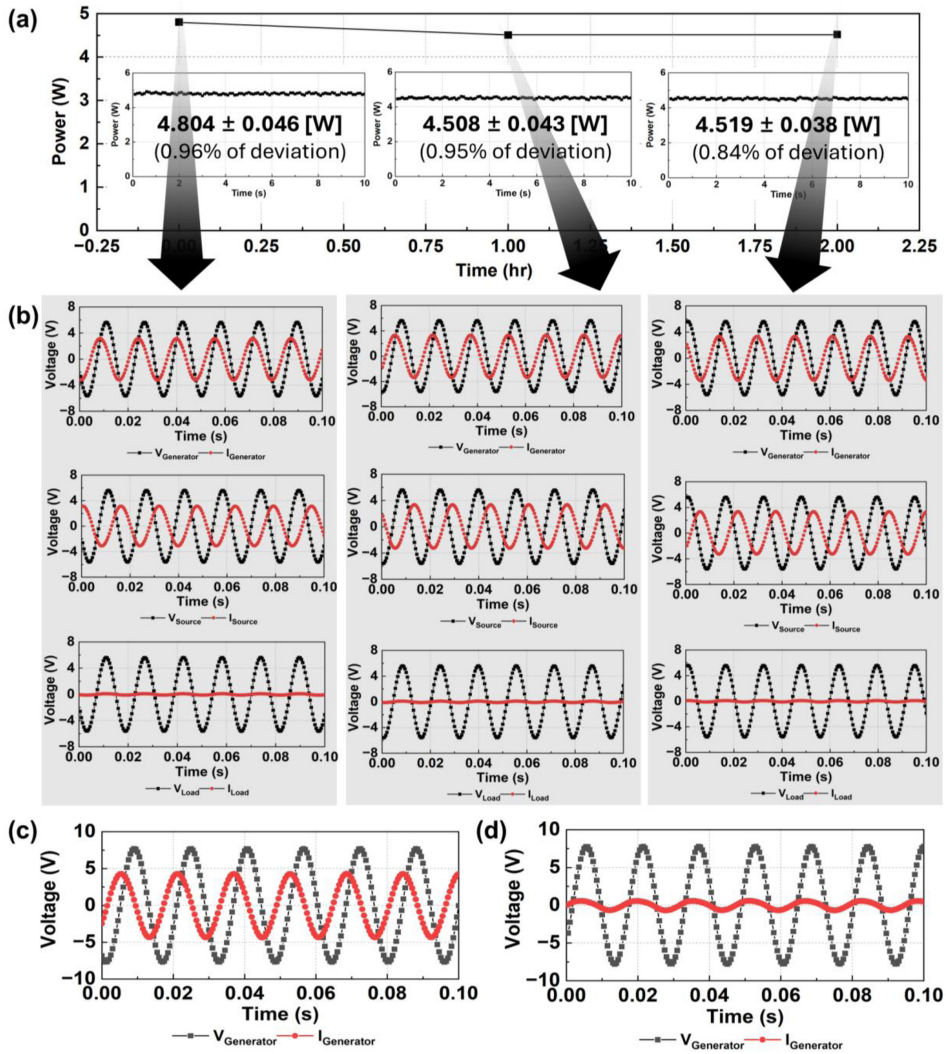

Fig. 4. Generation result, measured by the proposed system; (a) Measurement result of 2 h of continuous generation, (b) Detailed measurement results for AC voltage and current for each timestamp (Initial point, 1 h after start, 2 h after start), and detailed measurement results for (c) before threshold voltage and (d) after threshold voltage.

voltage, power, and current hot-end temperature (Fig. 3(a-iii)). Once the normal conditions are confirmed, the AC control panel initiates engine operation, with the driving frequency and amplitude defined as the operating parameters. The output voltage amplitude and power, both presented as RMS values, are monitored in the AC monitoring panel, whereas the Stirling monitoring section provides real-time data on the generated power (RMS value) and power factor.

The monitoring interface (Fig. 3(b)) provides more detailed measurements of the system parameters. Hot-end, coolant inlet, and outlet temperatures are recorded at 10 Hz to calculate ΔT (Fig. 3(b-i)), and the internal engine pressure is also tracked at 10 Hz (Fig. 3(b-ii)). The electrical power input/output of the Stirling generator, AC power supply, load, and power factor, are monitored at 10 Hz (Fig. 3(b-iii)). For higher-resolution analysis of the electrical circuit, the voltage and current signals are sampled at 2 kHz, which is approximately 15 times higher than the piston oscillation frequency (60–70 Hz), exceeding the Nyquist requirement to ensure precise waveform and power-transfer characterization (Fig. 3(b-iv)).

3. CONTROL AND MONITORING

To validate the proposed system, operational tests were conducted under the following conditions: helium pressure of 23 atm, hot-end temperature of ~560°C, cold-end temperature of ~3°C, AC power supply frequency of 63.6 Hz, amplitude of 5.6 V, and load resistance of 10 Ω. The engine was operated for two hours, with 10-second measurements taken at the initial start-up, after one hour, and after two hours. The results (Fig. 4(a)) show that the initial power output of 4.804 W decreased by approximately 6% to 4.508 W as the system

ⓒ The Korean Sensors Society

stabilized, with a measurement standard deviation of less than 1%. This gradual attenuation is attributed to natural thermal loss and temperature stabilization during long-term operation. Minor temperature fluctuations between the heater and cooler are believed to have contributed to the observed decrease. Fig. 4(b) presents the generator voltage and current waveforms recorded at 100 ms intervals, from which the output power was calculated. Simultaneous monitoring of the AC power supply and load signals confirmed the capability of the system to track real-time operation.

Amplitude sweep tests were performed by gradually increasing the AC power supply voltage. At amplitudes up to ~7.7 V, the system operated stably; however, once the threshold of ~7.8 V was exceeded, a significant drop in the output current was observed, leading to reduced power output (Fig. 4(c, d)). This phenomenon arises when the piston velocity exceeds the effective expansion velocity of the working gas (He) under the imposed ΔT, causing a phase shift between the pressure wave and piston motion. Consequently, the expansion force of the gas can no longer effectively support the piston motion, leading to a constant voltage but diminished current and conversion efficiencies. This behavior indicates the onset of a nonlinear damping regime in the FPSE, which will be addressed in future studies using a resonance-based impedance-matching circuit design.

4. CONCLUSIONS

In this study, a comprehensive control and monitoring system for a prototype Stirling generator was developed and validated experimentally. The system integrates precise internal pressure control, temperature gradient management, and high-frequency monitoring via LabView, enabling the synchronized acquisition of multiple variables, including pressure, voltage, current, and temperature. Using this platform, stable power generation was confirmed during long-term (2 h) operation, with the output decreasing from an initial 4.804 W to a stabilized value approximately 6% lower, while maintaining a measurement accuracy within 1% deviation. Furthermore, amplitude sweep tests revealed threshold behavior, wherein the output current sharply decreased beyond ~7.8 V, despite maintaining the voltage. This mode is attributed to the reduced force transfer efficiency owing to the mismatch between the piston speed and working gas expansion velocity.

These findings highlight two key areas for future research. First, impedance matching between the generator and load circuit must be implemented to suppress output degradation near the threshold conditions and improve operational stability. Second, although the heater temperature was used as a proxy for hot-end conditions in this study, the lack of perfect thermal insulation may have caused discrepancies between external heater readings and the actual internal ΔT of the generator. Therefore, improved insulation design and direct internal temperature sensing are required for more accurate thermal characterization.

Overall, the developed system provides a robust experimental platform for evaluating the Stirling generator performance and serves as a foundation for further optimization toward stable, high-efficiency operation in extreme environments.

CRediT Authorship Contribution Statement

Gujin Kang: Data curation, Formal analysis, Visualization, Writing – original draft. **Kilyoung Ko:** Investigation, Methodology, Writing – original draft. **Jongbum Kim:** Conceptualization, Investigation. **Jin-Joo Kim:** Conceptualization, Validation. **Sunjin Kim:** Conceptualization, Validation. **Jintae Hong:** Funding acquisition, Project administration, Supervision. **Yongrok Jeong:** Conceptualization, Data curation, Investigation, Methodology, Visualization, Writing – original draft, Writing – review and editing.

Declaration of Competing Interest

The authors declare that they have no known competing financial interests or personal relationships that could have appeared to influence the work reported in this paper.

Acknowledgements

This study was supported by the Kyungpook National University Research Fund (2025). This work was supported by the Korea Research Institute for Defense Technology Planning and Advancement (KRIT) grant funded by the Korea 310 government (DAPA, Defense Acquisition Program Administration) (22-107-C00-007) (KRIT-CT-23-055). This work was supported by a National Research Council of Science & Technology (NST) grant (a program for connecting researchers between the University and GRI).

REFERENCES

[1] G.T. Reader, C.H. Hooper, Stirling Engines, Elsevier, Oxford, UK, 1983.
[2] G. Walker, Stirling Engines, Clarendon Press, Oxford, UK, 1980.
[3] I. Urieli, D.M. Berchowitz, Stirling Cycle Engine Analysis, Adam Hilger, Bristol, UK, 1984.
[4] B. Kongtragool, S. Wongwises, A review of solar-powered Stirling engines and low temperature differential Stirling engines, Renew. Sustain. Energy Rev. 7 (2003) 131–154.
[5] P. Jimenez Zabalaga, E. Cardozo, L.A. Choque Campero,

ⓒ The Korean Sensors Society

J.A. Araoz Ramos, Performance analysis of a Stirling engine hybrid power system, Energies 13 (2020) 980.
[6] W.B. Nader, Methodology for the selection and optimization of energy converters for automotive powertrain applications, Ph.D. thesis, École Polytechnique, Palaiseau, France, 2019.
[7] M. Clark, Y. Lee, T. Hudson, J. Elliott, A. Davis, Comparison of radioisotope power systems to enable the endurance mission concept, Proceedings of 46th Int. IEEE Aerospace Conf., Montana, USA, 2025, pp. 1–10.
[8] M.R. Hanipah, R. Mikalsen, A.P. Roskilly, The real-time interaction model for transient mode investigations of a dual-piston free-piston engine generator, Appl. Therm. Eng. 2123 (2022) 118629.
[9] P.K. Yadav, S. Qiu, K. Yanaga, Design and development of test rigs for experimental investigation of flow loss and heat transfer in a Stirling engine heater head, Proceedings of AIAA Int. Energy Conv. Conf., Atlanta, USA, 2018, pp. 1–12.
[10] Y. Jeong, J.-B. Kim, S. Kim, J.-J. Kim, J. Kim, G. Kang, et al., Development of small-sized Stirling radioisotope generator, Proceedings of Nucl. Emerg. Technol. Space (NETS 2024), Santa Fe, New Mexico, USA, 2024, pp. 568–572.
[11] P. Durčanský, R. Nosek, J. Jandačka, Use of Stirling engine for waste heat recovery, Energies 13 (2020) 4133.

ⓒ The Korean Sensors Society